



In-situ

K C , W X , L ,*, L H , C , L , f L , s W , K s Ess , L L , X G , T P J^f

Gemological Institute, China University of Geosciences, Wuhan 430074, PR China
 Hubei Gem and Jewelry Engineering Technology Research Center, Wuhan 430074, PR China
 School of Materials Science and Engineering, Huazhong University of Science and Technology, Wuhan 430074, PR China
 Mechanical Engineering, University of Birmingham, Birmingham B15 2TT, UK
 School of Electrical and Electronic Engineering, Huazhong University of Science and Technology, Wuhan 430074, PR China
^fWMG, Materials Engineering Centre, University of Warwick, CV4 7AL Coventry, UK

ARTICLE INFO

Keywords:

T - s s l
 C s s ff l
 S l l s l
 C l s
 El f s l

ABSTRACT

C l , - s l (3DG) f s s l ss, s
 l s s ll s s l . H s l - s l -
 s s l l s l (SLM) f - s l (3D) s C
 l . G s in-situ l s (CVD) s C
 l , f 3DG s s . A f l CVD
 SLM f s ff l l s l f 3DG f -s ()
 , s ,) -s (X , s f l) s
 s ff l . T 3DG/ s ff l l 88% 27% l
 f (EMI) s l l ff s X s l . P SE f 32.3 B s EMI s l ffi-
 (SE) 47.8 B 2.7 GH X SE f 2-18 GH .
 T s s s l s s f f s f s
 l s s f SLM s s .

1. Introduction

G , s s f sp^2 s, s (2DG), X l s l s s 5 , s 6,7 ,
 s f (2630 2 -1) 1 , X ll s f , s s V s s f s (EMI) s l 8 s .
 (2 10⁵ 2 V⁻¹ s⁻¹) s s l s l f-ss l 11 , - ll 12 9 , l 10 ,
 (615000 W⁻¹ K⁻¹) 2 . H , s π - π s ff f s F X l , f
 s l (2D) s l - s s s f l s 13 . S l f-ss l
 ll, s ll, l , f l - l ss s s s l s f l l 14 . D - ll s s l ll
 3 . Af f s l s fi l ff s s 15 . M s s s f f l
 l s . C f s l s, - s l - s s l s s f f f l
 (3DG) s s s (99.7%), l s , l l - CVD s s s s , s
 s fi (0.6 -2) 4 s fi ll s s f l - l 16 . B
 s f s s ll s l , f s l s , s s l l
 ss sf s f - s l f l s s s s

*C s : G l l I s , C U s f G s s, W 430074, PR C .
 E-mail address: l@ . (. L).

s . T , X s s (. , s -
 s) , X fl fi s
 (. , l ss, f s) f 3DG. B s s, -
 3DG ll s f l l
 (. , s , s , s f l). H , s f s
 l l s l s ffi l
 s l l s , f s , l N f
 ll s s l ll f
 , s s l 3DG s s l f -
 s s s f s f s fi f l s 17,18 .
 H , s f ss l l s ,
 s l l f s s 3DG
 l s s s l f s 19 .
 S l l s l (SLM), s -
 f (AM) l , s l l s f f
 f s s / s X - s l (3D) l l s
 s f l X s , ffi
 fi X l f in-situ f l . T , s
 s s SLM s s s f T ll s 20 ,
 s l ss ll s 21 , N ll s 22 . C s s l s f l /
 s s f l - s s s - f - -
 s s l s . C N s s ,
 s s s l s s f
 CVD l s l (< 0.001 .%)
 ss s l f , -
 l s l l s 23 . W l N s
 s l l (> 0.1 .%) 17 , fi s
 f s f X ss 24 . H , -
 s SLM f s s ll s f s ffi
 f s l f s s l
 fl s l s l
 (1000-1100). F f s s s ff l s
 SLM s s ll f ll s 25 .
 T l s , f fi s s
 f s l - 3DG/ (3DG/C) s -
 s SLM s l s CVD f
 . A ll- s s l s
 ll s SLM f s l l -
 l -441(-250.7 s -288.5()-270375 s) 428TDlf l 16 --1.3020

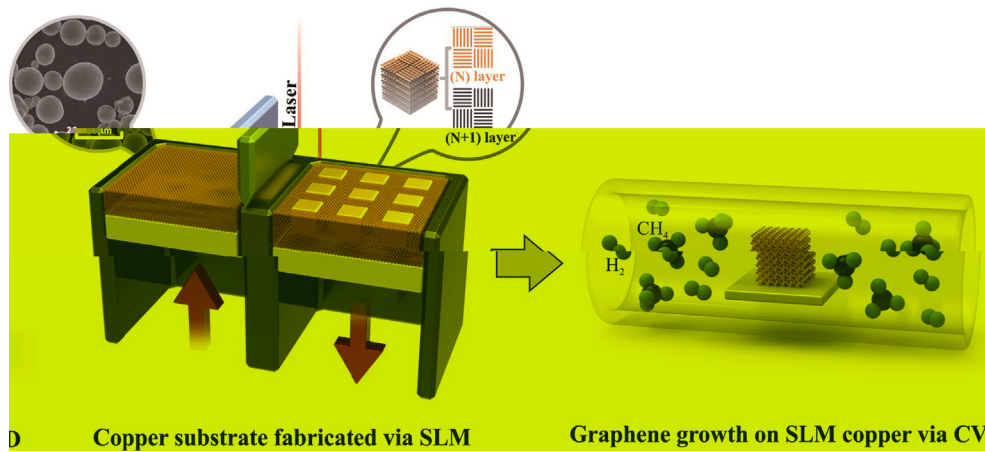


Fig. 1. SLM of copper substrate and in-situ growth of graphene on SLM copper via CVI.

ASTM B193-2002 (2010) and ASTM E1461-2013 (2013) for mechanical testing. The tensile strength of the SLM copper substrate was measured using a universal testing machine (LFA457, GOM) with a load cell of 50 N. The fracture surface was analyzed using a scanning electron microscope (SEM, S-4800, Hitachi) at 20 kV. The surface morphology was characterized using an atomic force microscope (AFM, SPM-A1500, Bruker) with a silicon cantilever (S11, S21, Bruker). The Raman spectra were recorded using a Renishaw inVia Raman microscope with a 633 nm laser line. The laser power was 400 mW and the scanning speed was 130 μm/s. The Raman spectra were fitted with Origin 8.5 software. The G and 2D bands were deconvoluted into three Lorentzian peaks. The intensity ratio of the G and 2D bands (I_{2D}/I_G) was used to evaluate the degree of graphitization. The results are summarized in Table 1.

3. Results and discussion

3.1. Formation of SLM copper

3.1.1. SLM manufacturing of copper under different line energy densities

The SLM process parameters were varied to study the effect of line energy density on the microstructure and properties of the SLM copper. The laser power and scanning speed were varied from 120 W to 200 W and 50 mm/s to 550 mm/s, respectively. The results are shown in Fig. 2.

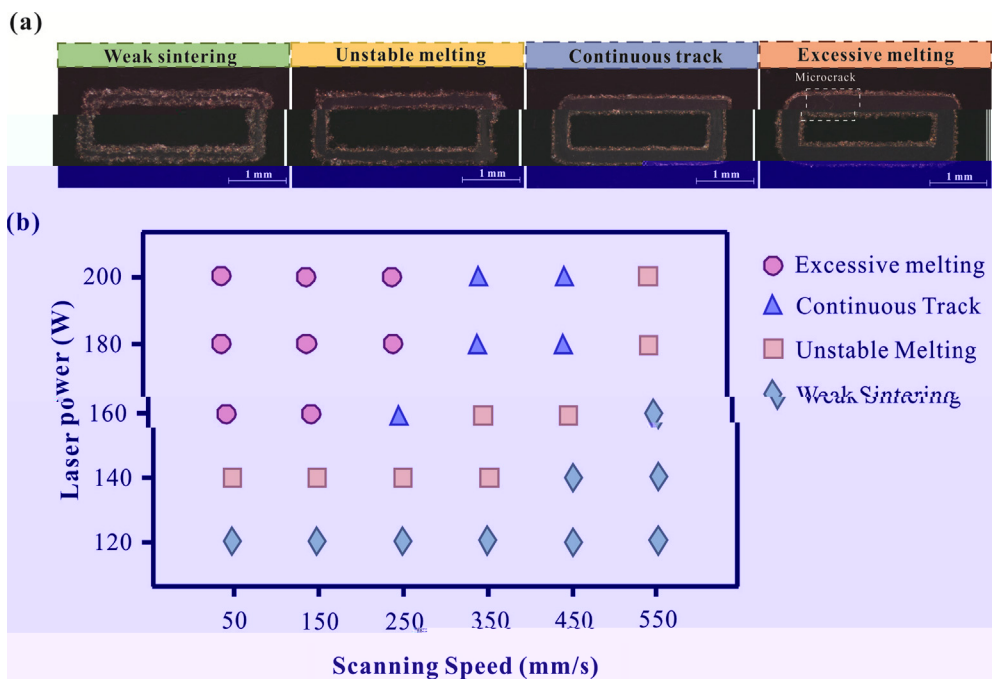


Fig. 2. (a) SEM images of SLM copper surfaces under different conditions. (b) Laser power vs Scanning Speed plot.

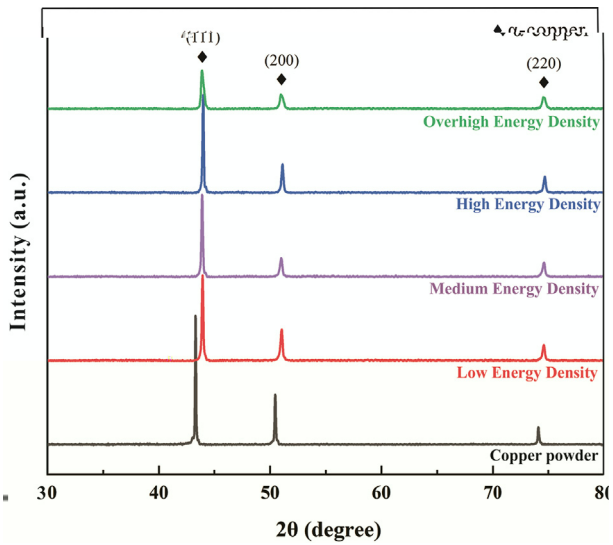


Fig. 3. XRD patterns of copper powder at different energy densities.

3.1.2. Formation of anisotropic microstructure under different volumetric energy density

The XRD patterns of copper powder at different energy densities are shown in Fig. 3. The intensity of the (111) peak increases with increasing energy density, indicating the formation of an anisotropic microstructure. The peak intensity ratio of (111) to (200) is used as a measure of the degree of anisotropy. The ratio is 1.0 for the copper powder, 1.1 for the low energy density, 1.2 for the medium energy density, 1.3 for the high energy density, and 1.4 for the overhigh energy density. The XRD patterns of the SLM samples are shown in Fig. 4. The intensity of the (111) peak increases with increasing energy density, indicating the formation of an anisotropic microstructure. The peak intensity ratio of (111) to (200) is used as a measure of the degree of anisotropy. The ratio is 1.0 for the copper powder, 1.1 for the low energy density, 1.2 for the medium energy density, 1.3 for the high energy density, and 1.4 for the overhigh energy density.

The XRD patterns of the SLM samples are shown in Fig. 4. The intensity of the (111) peak increases with increasing energy density, indicating the formation of an anisotropic microstructure. The peak intensity ratio of (111) to (200) is used as a measure of the degree of anisotropy. The ratio is 1.0 for the copper powder, 1.1 for the low energy density, 1.2 for the medium energy density, 1.3 for the high energy density, and 1.4 for the overhigh energy density. The XRD patterns of the SLM samples are shown in Fig. 4. The intensity of the (111) peak increases with increasing energy density, indicating the formation of an anisotropic microstructure. The peak intensity ratio of (111) to (200) is used as a measure of the degree of anisotropy. The ratio is 1.0 for the copper powder, 1.1 for the low energy density, 1.2 for the medium energy density, 1.3 for the high energy density, and 1.4 for the overhigh energy density.

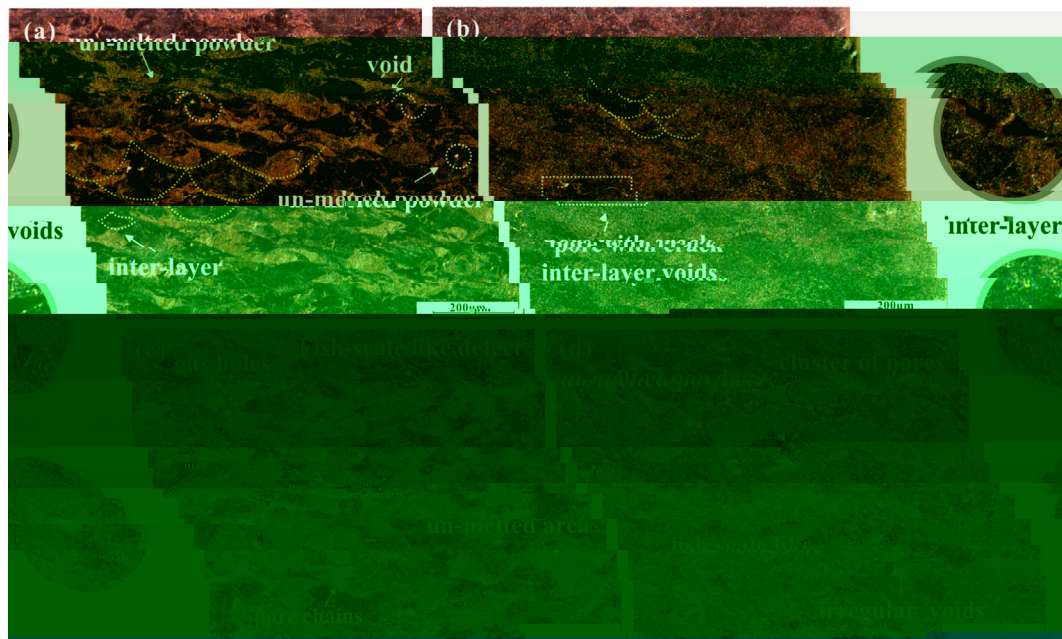


Fig. 4. SEM micrographs of SLM samples at different energy densities.

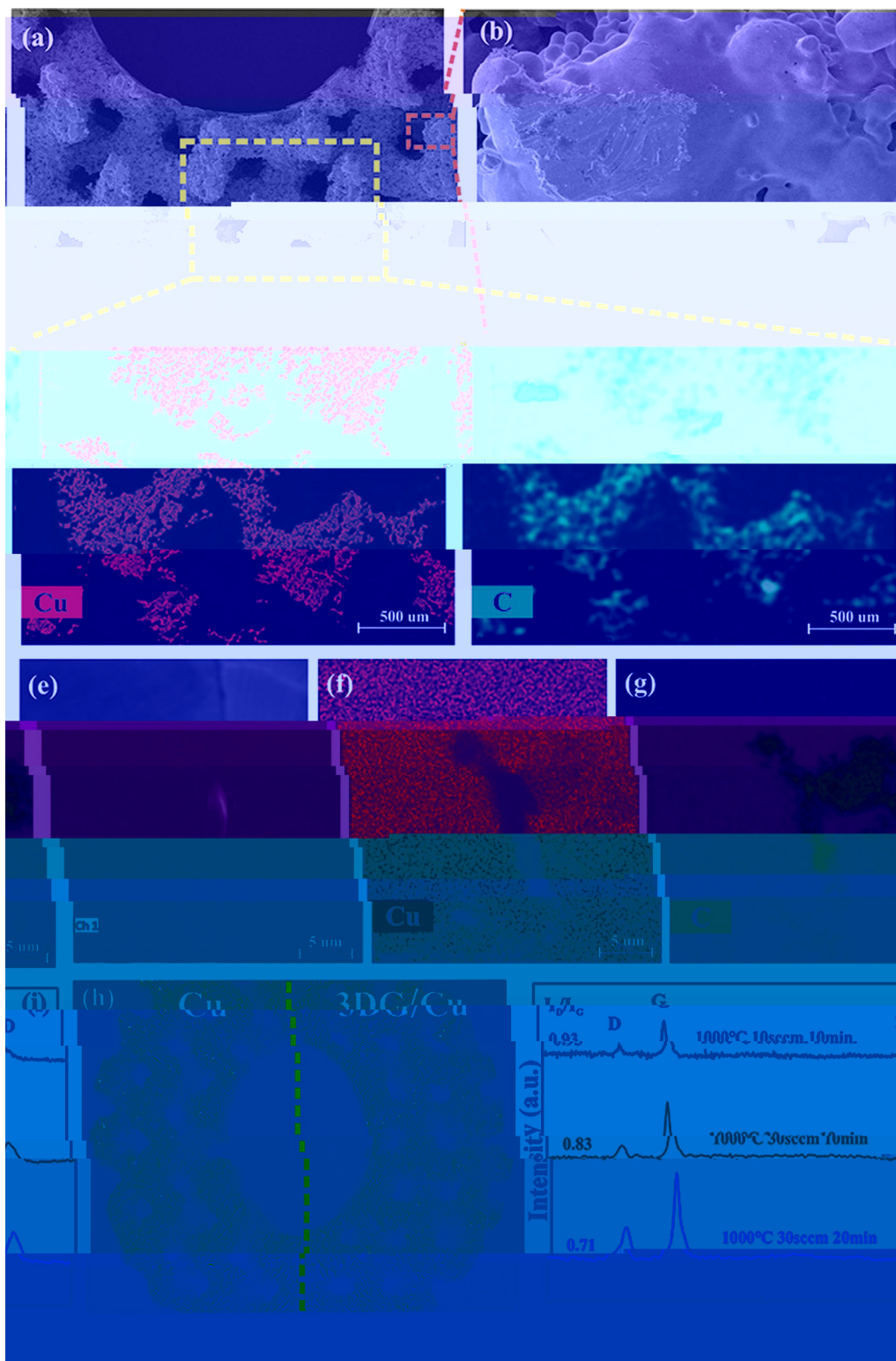


Fig. 8. (a) SEM image of the 3DG/Cu porous scaffold. (b) Magnified SEM image of the porous structure. (c) EDS map showing the distribution of Cu. (d) EDS map showing the distribution of C. (e-g) High-magnification EDS maps of Cu and C. (h) XRD patterns of 3DG/Cu scaffolds prepared at 1000°C for 30 min, 1000°C for 30 sec, and 1000°C for 10 min. The patterns show peaks corresponding to Cu and C, with intensity ratios of 0.71, 0.83, and 0.93 respectively.

3.4. Thermal property and EMI shielding effectiveness of 3DG/Cu porous scaffolds

The thermal stability of the 3DG/Cu porous scaffolds was evaluated by TGA. The TGA curves show that the scaffolds exhibit good thermal stability up to 1000°C. The weight loss of the scaffolds at 1000°C is 26.8% and 14.8% for the scaffolds prepared at 1000°C for 30 min and 1000°C for 30 sec, respectively.

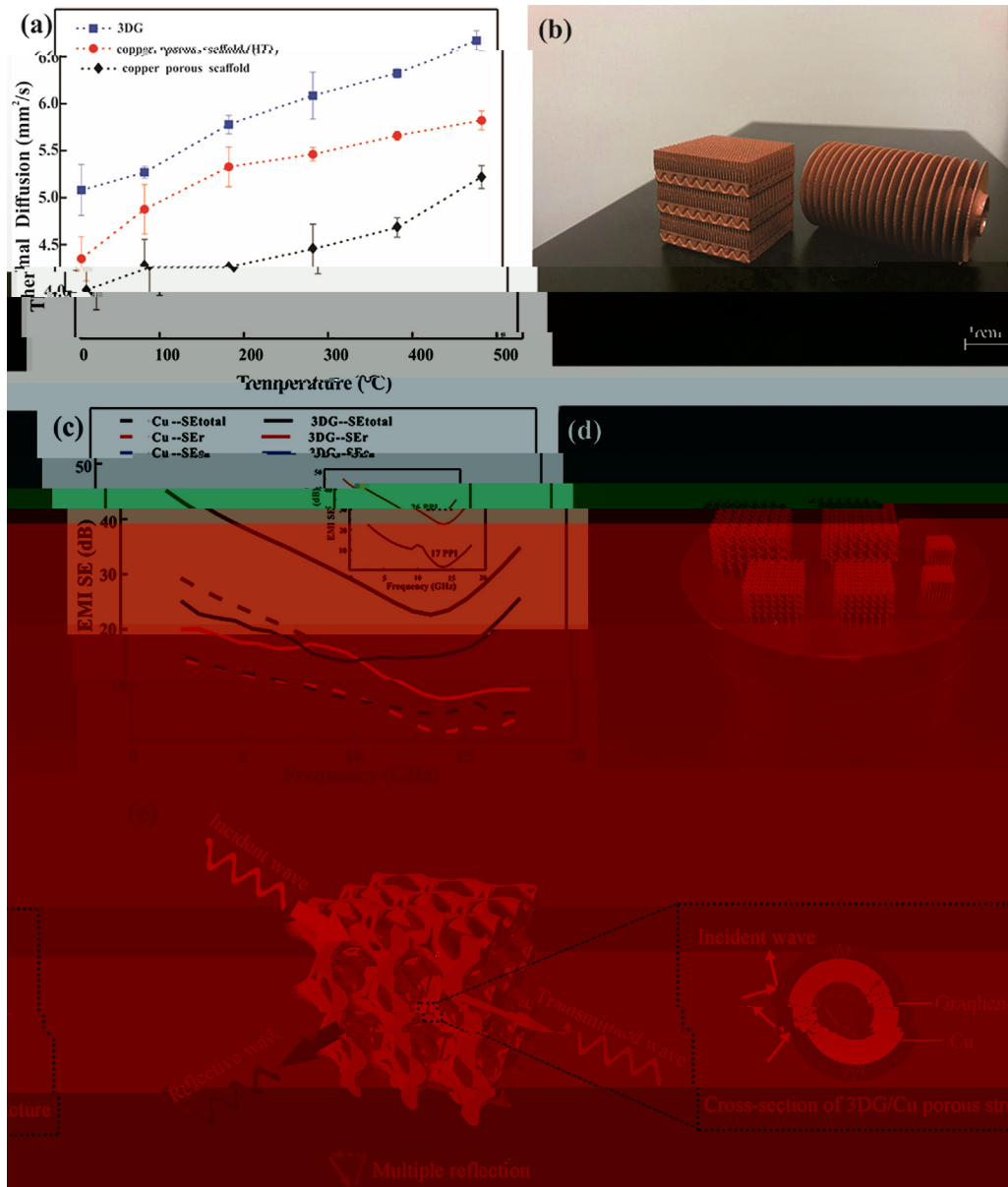


Fig. 9. P f f 3DG/C s s ff l : () l ff s ; () SLM s l ssff X (-s l fl l) f s s l s fi l , s f s f s l .) f 3DG/C EMI. (F

Table 1

Coating materials	Substrate	Method	Maximum shielding efficiency (dB)	Improvement of thermal property (%)	Ref
G	l s G	I s + f + l + l	37	-	50
G	PS	H - ss ss l + s l l	29.3	-	56
G	PMMA	S l l + l +	19	-	57
C /G	/C	S f fi + l l l	-	8.5	58
G	N	F + CVD	-	554	59
G	C -N	E l ss l + l s	20	-	60
G	C	P s + CVD	-	2.4	61
G	l s C	F - + l l	47	6.3	62
G	C	CVD + SLM	47.8	27	T s

Note: l (l l)-PPMA, l s -PS.

Declaration of Competing Interest

T s l s fl f s
l f s .

Acknowledgement

T s f ll l fi l s f
N l N l S F f C (N . 51671091, N .
51902295, N . 51675496). T
F l R s F s f C l U s s, C
U s f G s s (W) (N . (N . CUG170677) H
P N l S F (N . 2019 CFB264).

Appendix A. Supplementary data

S l s l f l s://
. /10.1016/ s s .2020.105904.

References

1 B RG, N N, M s K, M S. G : s l l f f
s s ss .P M S 2018;91:24-69.
2 B l AA, G s S, B W, C l, T l D, M F, l S
f s l l N L 2008;8(3):902-7.
3 L , H, C s M, P l H, P O, S l G, l I s X -
f l f s s f l s f f i l s l
s s. ACS A l M I f s 2016;8(36):24112-22.
4 K M, K J, J B, C , K JH, A JH. G - s - s l
s s f l l s. ACS N 2017;11(8):7950-7.
5 P , C M, H M, T M, , L D. P
s l f f - s l l l l
A l C l, B 2020;262:118266-76.
6 L XJ, W, C LL, J SH, W G, L, l, F l C-G f
l s s l
. C s P A
2017;101:50-8.
7 HQ, L SW, C LH, J SH, H HQ. S l f -
- f l - s. J M C A
2018;6(42):21216-24.
8 D s TM, S P, D s P, K J, K M, A s T, l. 3D -
- s- l l l l l l s f s l s
l l l l l l s f s l s
9 Q L, L L. T s f H . P C . P - s s s f s
s s f l l s s f l s X s .
RSC A 2014;4(72):38273-80.
10 D X, H L SP, N, W X JG. 3D
M S2 s : P l l l
f . C s P A 2016;90:424-32.
11 L XL, XW, S CO, H MK, X HL, D W , l S l f ss l -s ll
s f ll s s s 3D f l s fi EM -
s f . A F M 2018. s:// . /10.1002/ f .
201803938.
12 L J, P , X C, R G, , N l s D, l. G
s S O2 s s f l l s. ACS N
2013;7(7):6001-6.
13 J SH, A l S, G A. L - s ll l s s s f l
l s. A C I E 2017;56:15520-38.
14 I , T , S K, K s M, T s T, T K, l. T -
s l l s s l
s. PCCP 2018;20(9):6024-33.
15 S K, D N, M ll C, V s l N, E l J. T ll l
l J E l S 2002;149(8):370-7.
16 C XH, S M, S WH, L G, H X, Q , l P f l 3D
l X s f s s. S ll 2011;7(22):3163-8.
17 K s H, G X M, J s l, H J, W C, C M. U l -
f s l f - s l - s
. M 2019;1(4):1077-87.
18 S Q, F, X, L W, L H, L , l C - l l
- s ll l f s f l - f - l l
f l s l . A M 2017;29(31):1701583-90.
19 X X, G C, X L, T H, D, W , l. T s ll f -
f l f s s s f
s. ACS N 2019. s:// . /10.1021/ s .9 08191.
20 C C, H , B X, N J, C S, L F, l. 3D s T 6A l 4V :
ff s f l s f l ;
l M D s 2019;175:107824-33.
21 S š c J, B ž c D. T ff f NB s f l -
s f 316L s ll s l s l s SLM. S f C
T l 2016;307:407-17.

22 R DC, HB, L J, L SJ, J W, R, l M s
f T-N ll f s l l s l . M S E A-S
2020;771:138586-95.
23 L X, C W, A J, K S, N J, D, l L - s s s f - l
f f l s f l s. S 2009;324(5932):1312-4.
24 C P, R WC, G LB, L BL, P SE, C HM. T - s l f l l
s . N M 2011;10:424-8.
25 J SD, D s S, G ss s L, K JP, H X JV, V s l K.
I fl f s l l s l ss s X l
. J M P ss T l 2019;270:47-58.
26 X W, H L, L , T D, C Q, F , l. Eff (s l l s l
s s s l , s fi
s f s s ll . M D s 2019;170:107697-708.
27 G DD, M s W, W ss K, P R. L s f f
ll s: l s, ss s s. I M R
2013;57(3):133-64.
28 L E, T s S, C s L, F A. Eff (s l l s l (SLM)
ss s s s f 316L s
s ll s s l J M P ss T l 2017;249:255-63.
29 X , S, W , L J, W P, C , l. F f l s s f
s l s s l l s l f T 6A l 4V. A l P s A: M S
P ss 2018;124:685-98.
30 L , M, S, D W, S C. I s s
s l l s l f A l S 316L s ll s s l . M D s
2015;87:797-806.
31 L CLA, M ss S, T M, A RC, W s PJ, L PD. T ff f
f f f l s f . A M
2019;166:294-305.
32 T X, K , T WQ, T J, D s s M, M l D, l. R l -
s s f α/β f l l
s l T -6A l 4V. S R 2016;6:26039-48.
33 K H, T XP, L NH, T SB, C CK. G f s
ss f s l l T -6A l 4V s. V l
P s P 2016;11(3):183-91.
34 R fi HK, K NV, G H, S TL, S BE. M s s l
l . J M E P f 2013;22(12):3872-83.
35 T X, K , T J, V s l G, P QX, G, l. A X l
s l T -6A l 4V. J A ll s C 2015;646:303-9.
36 R DA, M LE, M H , l. N l - s l
f l f f s l
f s l l . A M 2011;59(10):4088-99.
37 s , X, W H. Eff f s ll s
s f s l l s l C -2.4N -0.7S ll . J A ll s C
2018;743:258-61.
38 K S. W ll . S E 2003;23:309-48.
39 L G , G s J ff R, G s N P. E l C (111). N
L 2010;10(9):3512-6.
40 L XS, C WW, C l , R ff R S. E l f
C s l . N L 2009;9(12):4268-72.
41 XW, X C, X, W H, SQ, L. A s l l l l l -f
f s f s f s. C
2020;161:479-85.
42 F AC, M JC, S V, C s C, L M, M F, l R
s f s P s R L 2006;97(18):187401-4.
43 S , G , J SH, F PC, H HQ. F l l f l
- l s fi s l l
M L 2017;200:97-100.
44 J K, H, J, C J, D . F l l f
s l f f - ll f f C -N ll CNTs.
A l S f S 2014;311:351-6.
45 R š c K, M l DP, A s C, M S, S š K. X ll EMI s l
l s l l s l
- s s f s. C s P A 2018;12:475-84.
46 S B, L , W, W. C ss l - f s
l l s f š s l l f (EMI) s l . ACS
A l M I f s 2016;8(12):8050-7.
47 L N, H , D F, H X, L X, G N ((H)-305.3(X)-30228(L)-278J9.3 l)-340.5(S 0-3

M 2019;34(5):489–98.

53 W B, C M, L M. R s: l - - ffi
 l f s l l s. A M
 2014;26:3484–9.

54 C H, W S, J , J, X X, C J, l. S ff f F₃O₄
 l s fl l l (l fl) s fl s
 ss l s l . C s P A
 2019;121:139–48.

55 W L, J, Q. T ff f MWCNTs l -
 s f f -MWCNTs s s. J M S : M E l
 2015;26(3):1895–9.

56 D X , P GR, H P, Q F, M B , ML. Effi l
 f s l fl / l s s . J. M
 C 2012;22:18772–4.

57 HB, Q, WG, H X, . T - l ll l
 f s f l f s l . ACS A l M I f s
 2011;3:918–24.

58 S A, U ll N, T l f V. T l l f
 l - ll s f s l s f
 M f R 2016. s:// . /10.1051/ f /2016021.

59 P s MT, J H, R ff RS, S L. T l s - s l f -
 s f f l l . N L
 2012;12:2959–64.

60 J K, H, H , D . P f f - ll f f C -N ll -
 s s l s l f . M L
 2017;122:244–7.

61 R H, L S, B S, K TW, L DS, L HJ, l. T - s l s
 - s s s
 f . S R 2015. s:// . /10.1038/s 12710.
 ss -

62 XT, F SG, L , G Q, L G, R KP, l. S s l X -
 l f s l l
 s s s 3D s/ ll l
 l f . M S E A-S 2020. s:// . /10.1016/j
 s s .2019.105670.

63 R DA, M LE, M E, H DH, M JL, M BI, l.
 N l - s l f f s l
 s s f s l l . A
 M 2011;59(10):4088–99.

64 E s SF, L KG, S s VK, M IC. T l l s f . J T s
 E l 1973;1(1):10–38.